



Bioactive skin-mimicking hydrogel band-aids for diabetic wound healing and infectious skin incision treatment

Yuxuan Yang^{a,1}, Xiaodan Zhao^{a,1}, Jing Yu^b, Xingxing Chen^b, Ruyue Wang^b, Mengyuan Zhang^b, Qiang Zhang^b, Yanfeng Zhang^b, Shuang Wang^a, Yilong Cheng^{b,*}

^a Key Laboratory of Shaanxi Province for Craniofacial Precision Medicine Research, College of Stomatology, Xi'an Jiaotong University, Xi'an, 710049, China

^b School of Chemistry, Xi'an Jiaotong University, Xi'an, 710049, China

ARTICLE INFO

Keywords:

Hydrogel
Tannic acid
Wound dressing
Chronic diabetic wound
Hydrogen bonding

ABSTRACT

The treatment of diabetic chronic wounds remains a global challenge due to the up-regulated inflammation response, oxidant stress, and persistent infection during healing process. Developing wound dressing materials with ideal biocompatibility, adequate mechanical strength, considerable under-water adhesion, sufficient anti-inflammation, antioxidant, and antibacterial properties is on-demand for clinical applications. In this study, we developed a bioactive skin-mimicking hydrogel band-aid through the combination of tannic acid (TA) and imidazolidinyl urea reinforced polyurethane (PMI) (TAP hydrogel) and explored its potentials in various medical applications, including hemostasis, normal skin incision, full-thickness skin wounds, and bacterial-infection skin incision on diabetic mice. TA was loaded into PMI hydrogel network to enhance the mechanical properties of TAP hydrogels through multiple non-covalent interactions (break strength: 0.28–0.64 MPa; elongation at break: 650–930%), which could resist the local stress and maintain the structural integrity of wound dressings during applications. Moreover, owing to the promising moisture-resistant adhesiveness and organ hemostasis, outstanding anti-inflammation, antibacterial, and antioxidant properties, TAP hydrogels could efficiently promote the recovery of skin incision and defects on diabetic mice. To further simulate the practical situation and explore the potential in clinical application, we also verified the treatment efficiency of TAP hydrogel in *S. aureus*-infected skin incision model on diabetic mice.

1. Introduction

With the worldwide prevalence of diabetes mellitus, chronic wounds with persistent hyperglycemia, upregulated inflammatory reaction, and bacterial infection pose a serious threat to the prognosis as well as the life quality of diabetic patients [1]. Diabetic microangiopathy is the most common complication of hyperglycemia which could compromise the barrier function of skin, and cause delayed wound healing [2]. Conventional methods for chronic wound treatment like wound debridement and dressing provide limited therapeutic effect, and cannot meet the diversified demands of diabetic wound healing [3].

Wound dressing is regarded as an effective way for the treatment of wounds in the clinic. The wound healing process can be divided into four distinguished phases, including hemostasis, initial inflammatory response, cell proliferation, and tissue remodeling [4]. Therefore, an

ideal wound dressing material should be functionalized as the skin tissue which serves as a physical boundary to protect the vulnerable internal environment and feature desirable therapeutic effects towards wound healing phases. Biocompatible wound dressing materials with multi functionalities, such as electrospun nanofibers [5], microfiber networks [6], membrane [7], and hydrogels [8] have been employed for skin tissue imitation, which can cover exposed tissue, avoid body fluid evaporation, and provide extra protection for the wound area [9]. However, the disadvantages of current wound dress materials have been substantially revealed during research and clinical application, for instance, poor antibacterial capability [10], lacking anti-inflammation property [11], undesirable mechanical strength [12], and weak adhesive ability to body fluid stained surfaces [13], especially in the treatment of diabetic patients who suffer from chronic wounds or infection [14].

Peer review under responsibility of KeAi Communications Co., Ltd.

* Corresponding author.

E-mail address: yilongcheng@mail.xjtu.edu.cn (Y. Cheng).

¹ These authors contributed equally to this work.

<https://doi.org/10.1016/j.bioactmat.2021.04.007>

Received 8 January 2021; Received in revised form 28 March 2021; Accepted 6 April 2021

2452-199X/© 2021 The Authors. Publishing services by Elsevier B.V. on behalf of KeAi Communications Co. Ltd. This is an open access article under the CC

BY-NC-ND license (<http://creativecommons.org/licenses/by-nc-nd/4.0/>).

The uncovered and moist wound surface with nutritious body fluid leakage provides an ideal environment for microbe settlement [15]. On account of persistent hyperglycemia, diabetic wounds exhibit excessive inflammation reactions and thus are beneficial to bacteria colonization, which could lead to a significantly prolonged wound healing process [16]. More importantly, the immunity of diabetic patients is also compromised and the diabetic chronic wound usually suffers from infections before proper treatment, which is the main reason for diabetic amputations [17]. With the constant increasing incidence of diabetic chronic wounds worldwide, a skin-mimicking wound dressing material with multiple functions including adequate mechanical strength, antibacterial, antioxidant, anti-inflammation, and tissue adhesive properties is on-demand for diabetic wound cover and rapid healing.

In our previous work, we developed a series of hydrogen bonding supramolecular hydrogels (PMI hydrogels), which are composed of poly (ethylene glycol) (PEG), methylene diphenyl 4, 4-diisocyanate (MDI), and imidazolidinyl urea (IU) [18]. PMI hydrogels presented similar mechanical strength as human soft tissue and exhibited excellent in vitro/in vivo biocompatibility, which has been used as an efficient physical barrier for the prevention of postoperative adhesion. However, due to the limited bioactivity, it is not suitable as a wound dressing for chronic diabetic wound healing. Tannic acid (TA), a plant-derived natural polyphenol, shows promising anti-inflammation, antibacterial, and antioxidant properties, which have been widely investigated for various applications [19]. Owing to 25 phenolic hydroxyl groups, TA can cross-link hydrophilic macromolecules, such as poly (ethylene glycol) (PEG) [20], poly (vinyl alcohol) (PVA) [21], and poly (N-hydroxyethyl acrylamide) (PHEAA) [22], to form a hydrogel network through multiple hydrogen bonding and hydrophobic interactions. Hence, we speculate that the introduction of TA into PMI hydrogels may endow it with desired functions as wound dressings, among which TA can further crosslink the hydrogel network through the interaction with ether, urethane, and benzyl groups.

In this work, we combined the advantages of PMI hydrogel and TA to construct bioactive skin-mimicking hydrogel band-aids for various applications (Scheme 1a), including hemostasis, anti-infection, wound defect healing, and skin incision treatment on diabetic mice. PMI was first synthesized through the hydroxyl-isocyanate chemistry as shown in Scheme 1b, and TA loaded PMI hydrogels (TAP hydrogels) were then prepared by soaking the PMI film into TA solution (Scheme 1c). Compared with the multiple synthetic steps for previously reported skin-mimicking hydrogels [23], all the raw materials in our work are commercially available and the preparation process of TAP hydrogels was facile. Owing to the multiple non-covalent interactions between PMI and TA (Scheme 1d), TAP hydrogels should feature improved mechanical properties compared to PMI hydrogels. Additionally, the presence of catechol groups endowed the TAP hydrogels with promising under-water adhesiveness and organ hemostasis. We carefully established the in vitro antibacterial and antioxidant effects of TAP hydrogels, and evaluated the potentials in the treatment of normal skin incision, full-thickness skin wounds, and bacterial-infection skin incision on diabetic mice. TAP hydrogels with desired mechanical properties, adequate adhesiveness, and multiple therapeutic effects may act as potent wound dressings for various wound healing in clinic.

2. Result and discussion

2.1. Characterization of TAP hydrogels

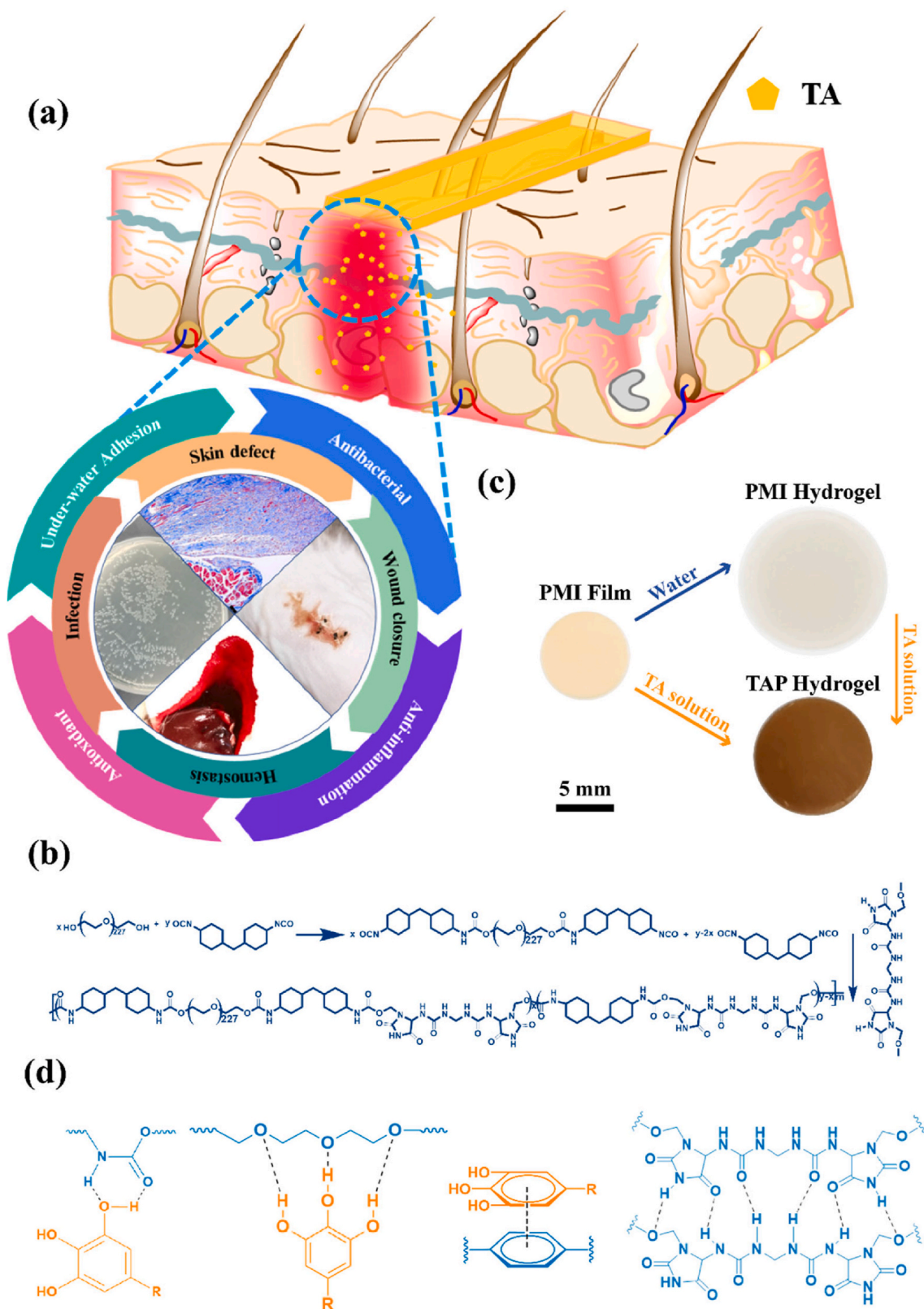
TAP hydrogels were prepared by two steps: PMI was first synthesized by polycondensation of PEG₁₀₀₀₀, MDI, and IU in the presence of DBTDL with the molar ratio of 0.3:1.7:2 according to our previous work [18]. The PMI dry films were soaked in TA solutions with different concentrations to afford the TAP hydrogels. TA was loaded into hydrogel matrix through the multiple non-covalent interactions (hydrogen bonding and hydrophobic interaction) [19]. TAP hydrogels prepared in 10%, 20%

and 30% TA solutions were termed as TAP10%, TAP20% and TAP30%, respectively. It was found that the drug loading efficiency gradually increased with the extension of incubation time, and it reached the plateau after 96 h of soaking (Fig. S1). It should be noted that there was no obvious weight loss for PMI hydrogel when it was incubated with water for 4 days (Fig. S2). The brown and transparent hydrogel films were obtained as shown in Fig. S3, and the higher TA concentration led to the smaller size of TAP hydrogels. After lyophilization, the TA content was measured. With the increase of TA concentration, the drug loading efficiency increased from 108% to 116% (Fig. S4). Scanning electron microscopy (SEM) results showed that the reduction of the pore size in the microstructure was observed in TAP hydrogels network compared to that in PMI hydrogel (Fig. 1a and Fig. S5). As shown in Scheme 1d, hydrogen bonds between urethane or ether groups in PMI and hydroxyl groups in TA as well as hydrophobic interaction can be formed with the introduction of TA. We then performed FT-IR to investigate the formation of hydrogen bonds between PMI and TA. As shown in Fig. S6, compared with TAP30% hydrogel, the C=O and O–H stretch in TA shifted from 1702 to 1710 cm⁻¹ and 3340 to 3379 cm⁻¹, respectively, and the stretching vibration of –CH₂ in PMI shifted from 2926 to 2918 cm⁻¹, all of which indicated that the formation of hydrogen bonds between PMI and TA [20,21b]. The increase of the TA concentration should lead to the formation of more non-covalent interactions, which were contributed to the improved drug loading, enhanced crosslinking density of the network, and the change of morphologies of the hydrogels macroscopically and microscopically [19].

The in vitro degradation of PMI and TAP30% hydrogels was performed in the presence of lipase and the results were shown in Fig. S7. It was found that gradual weight loss was detected for both PMI and TAP30% hydrogels, and the degradation rate of TAP30% hydrogel was slower than that for PMI hydrogel, which was due to the enhanced crosslinking density of TAP30% hydrogel network. After 21 days, PMI hydrogel can be completely degraded compared to around 25% weight remaining for TAP30% hydrogel. Moreover, the in vitro TA release of TAP hydrogels was tested by UV–Vis spectrophotometer. As depicted in Fig. S8, around 80% of TA was released in the first 3 days, which is essential for the suppression of the initial inflammation reaction as well as preventing bacterial colonization [24]. The higher TA loading efficiency, the slower release rate, which was attributed to the denser of the hydrogel network. The sustained TA releasing period can last up to 11 days, which covered most of the wound healing time. Prolonged and sustained release of TA makes TAP hydrogels reliable on anti-inflammation and antibacterial applications as bioactive wound dressings [25]. We also tested TA release in the presence of enzyme, and the accelerated release rate was observed as shown in Fig. S9, which was due to the degradation of TAP30% hydrogel.

2.2. Mechanical properties of TAP hydrogels

As the largest tissue organ in human body, skin undergoes various deformation in human activity and can protect the human body from external damage. Hence, as a powerful skin wound dressing, it should feature similar mechanical properties as human skin tissue. After TA loading, the mechanical properties of TAP hydrogels were evaluated by tensile testing. It was found that the tensile strength and elongation of TAP hydrogels increased as TA concentration increased from 10% to 30% (Fig. 1b), which was consistent with the reduced size of the microstructure observed by SEM. The stress-strain curves demonstrated that the break strength of TAP hydrogels was in the range of 0.28–0.64 MPa compared to 0.15 MPa for PMI hydrogel, while the elongation at break of TAP10%, TAP20%, and TAP30% hydrogel increased to 650%, 870%, and 930%, respectively. It has been reported that the combination of TA and other macromolecules (such as PVA, gelatin) could significantly improve the stretchability of the resulting hydrogels [21]. Since the hydrogen bonds formed between PMI and TA are relatively weak and prone to break, TAP hydrogels feature promising elongation



Scheme 1. (a) Schematic illustration of the anti-infection, wound healing, incision closure, and hemostasis functions of TAP wound dressing hydrogels. (b) Synthetic routes of the PMI carrier network. (c) Digital photographs and schematic preparation of the PMI film, water swelled PMI hydrogel, and TA loaded TAP hydrogels. (d) The possible non-covalent interactions within TAP hydrogels.

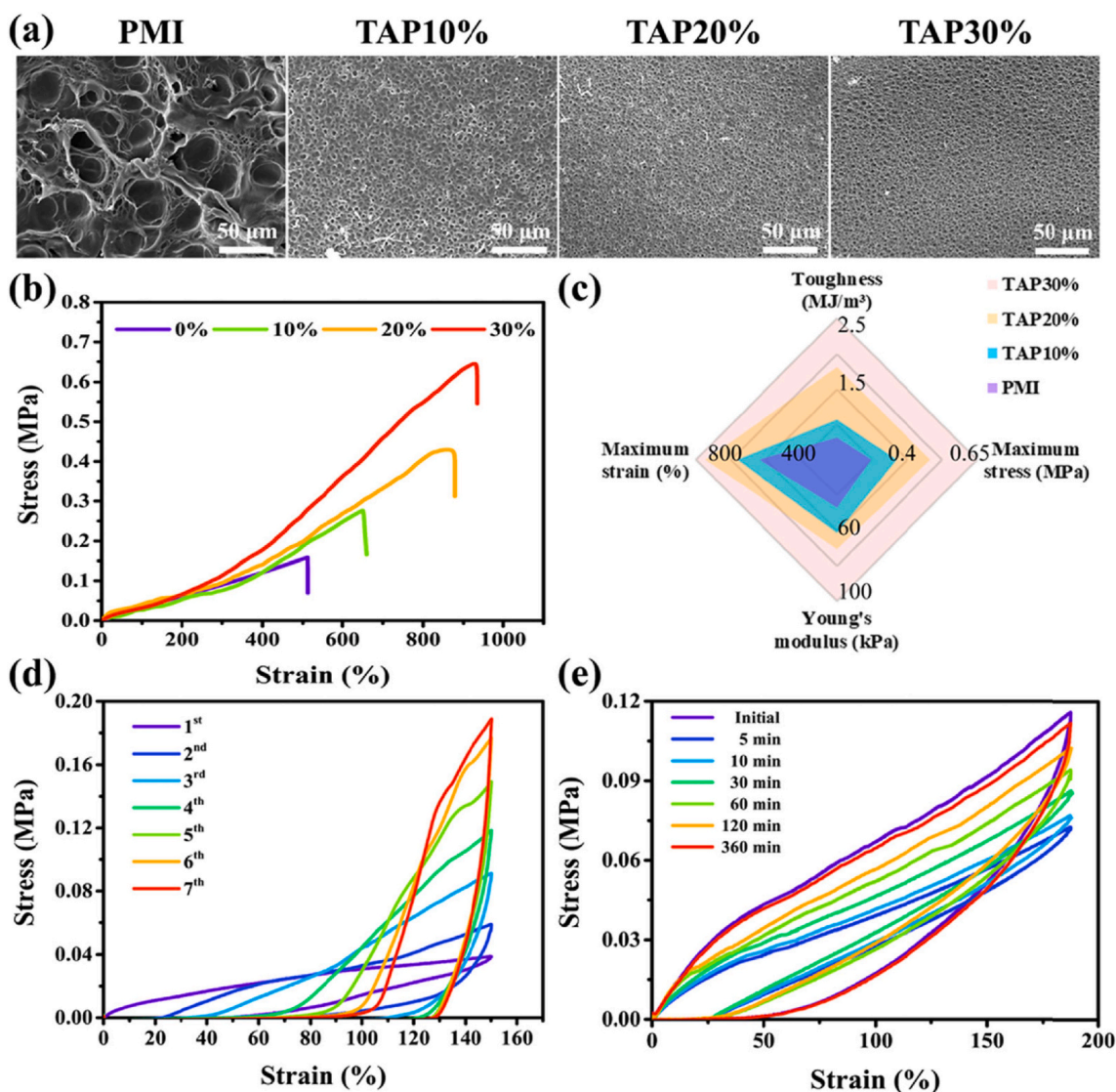


Fig. 1. Microscopic morphology, mechanical properties, anti-fatigue, and self-recovery properties of TAP hydrogels. (a) SEM photographs of PMI and TAP hydrogels loaded with different concentrations of TA solution (10%, 20%, 30%). (b) Tensile stress-strain curves of PMI, TAP10%, TAP20%, and TAP30% hydrogels (crosshead speed 50 mm min^{-1}). (c) Summaries of toughness, elongation at break, Young's modulus, and breaking stress of PMI, TAP10%, TAP20%, and TAP30% hydrogels. (d) Stress-strain curves of cyclic fatigue resistance testing of TAP 30% hydrogel. (e) Self-recovery behaviors of TAP 30% hydrogel with different resting times (5, 10, 30, 60, 120, and 360 min).

compared to PMI hydrogel. The stretchability of human skin is known to be 20–180% [26], and the wide deformability of TAP hydrogels can meet the demand for artificial human skin and bear external or local stress for applications. Moreover, we found that the toughness of the TAP hydrogels increased sharply to 0.7, 1.7, 2.6 MJ m^{-3} , which was 1.8, 4.3, and 6.5 times of that by PMI hydrogel (Fig. 1c). The Young's modulus of TAP hydrogels can reach 102 kPa when PMI was soaked in 30% TA solution, and this value is equivalent to that of human skin [24a, 27]. In addition, further increase of TA concentration led to the decline of mechanical strength (TAP40%, Fig. S10), which may be due to the increased rigidity of the network with higher hydrogen bonding interaction [28]. We also performed the mechanical test of TAP hydrogel at different time intervals during the release study. As shown in Fig. S11, the mechanical strength of TAP hydrogels decreased with TA release. After 3 days, the break strength was reduced to around 30% of the initial one. Hence, TAP hydrogels with excellent mechanical properties may show vast potential as artificial skin-mimicking materials [29].

Human tissue like skin or alimentary canal undergoes constant movement, and thus an ideal wound dressing material should possess

sufficient anti-fatigue property which allows it to maintain mechanical strength as well as structural integrity for practical applications. Hence, cyclic tensile loading-unloading tests with a maximum strain of 150% were employed to evaluate the capability of the anti-fatigue property of TAP30% hydrogel. As expected, the anti-fatigue ability was also reinforced after TA loading. As shown in Fig. 1d, for the first cycle, a large hysteresis loop with 20.0 kJ m^{-3} energy dissipated was observed for TAP30%. Compared to the decrease in the hysteresis loop and dissipated energy by PMI hydrogel (Figs. S12a and S12b), both of them gradually increased for the next three cycles as well as the improvement of the stress for TAP30% hydrogel (Fig. S12c), which may be attributed to the reconstruction of hydrogen bonding interaction between TA and PMI. After four cycles, the dissipated energy tended to be stable and did not show obvious decline even the loading-unloading cycle was processed seven times. Next, the self-recovery efficiency of TAP hydrogels was evaluated by successive load-unloading test after resting for pre-determined time intervals. As presented in Fig. 1e, with the increase of resting time, TAP30% hydrogel gradually recovered, and almost 100% recovery efficiency was detected after resting for 360 min. The same

trends were also observed for TAP10% and TAP20% hydrogels (Figs. S12d and S12e), indicating promising self-recovery behavior by TAP hydrogels. These results suggested that TAP30% hydrogel possessed outstanding anti-fatigue and self-recovery abilities and should be a good candidate for wound dressing application.

2.3. Adhesive property evaluation

The adhesiveness to the wound surface is an essential factor for wound dressings design, which can make ease of the clinical operation. The incorporation of TA into PMI hydrogel endowed TAP hydrogels with excellent adhesiveness with different substrates attributed to the catechol groups [30]. The adhesive property of TAP hydrogels was thoroughly studied by lap shear test and under-water adhesion demonstration. As shown in Fig. 2a, TAP10%, TAP20%, and TAP30% hydrogel exhibited a medium adhesive strength of 21.7 kPa, 31.6 kPa, and 35.4 kPa with the glass substrate, respectively. The more robust

adhesive strength was found between TAP hydrogels and porcine skin, and the average adhesive strength of TAP10%, TAP20%, and TAP30% hydrogel increased to 32.3 kPa, 49.4 kPa, and 68.2 kPa (Fig. 2b), respectively. A video demonstration of adhesion property between TAP30% hydrogel and mice skin was also shown in Movie S1.

Supplementary video related to this article can be found at <https://doi.org/10.1016/j.bioactmat.2021.04.007>.

Furthermore, the adhesive behavior of TAP30% hydrogel to the main organs of mice was tested (Fig. 2c). It was found that 8 major organs of C57 mice (heart, lung, liver, spleen, stomach, kidney, bladder, and gastrocnemius) can firmly adhere to TAP30% hydrogel. This wide array of adhesion on target tissues provides ubiquitous potentials for medical applications.

As the wound site is commonly covered with body fluid, the underwater adhesive ability is a desirable function for wound dressing hydrogels. As shown in Fig. 2d and e, Movie S2, and S3, TAP30% hydrogel (2 cm × 2 cm) could easily lift a 500 g weight underwater from

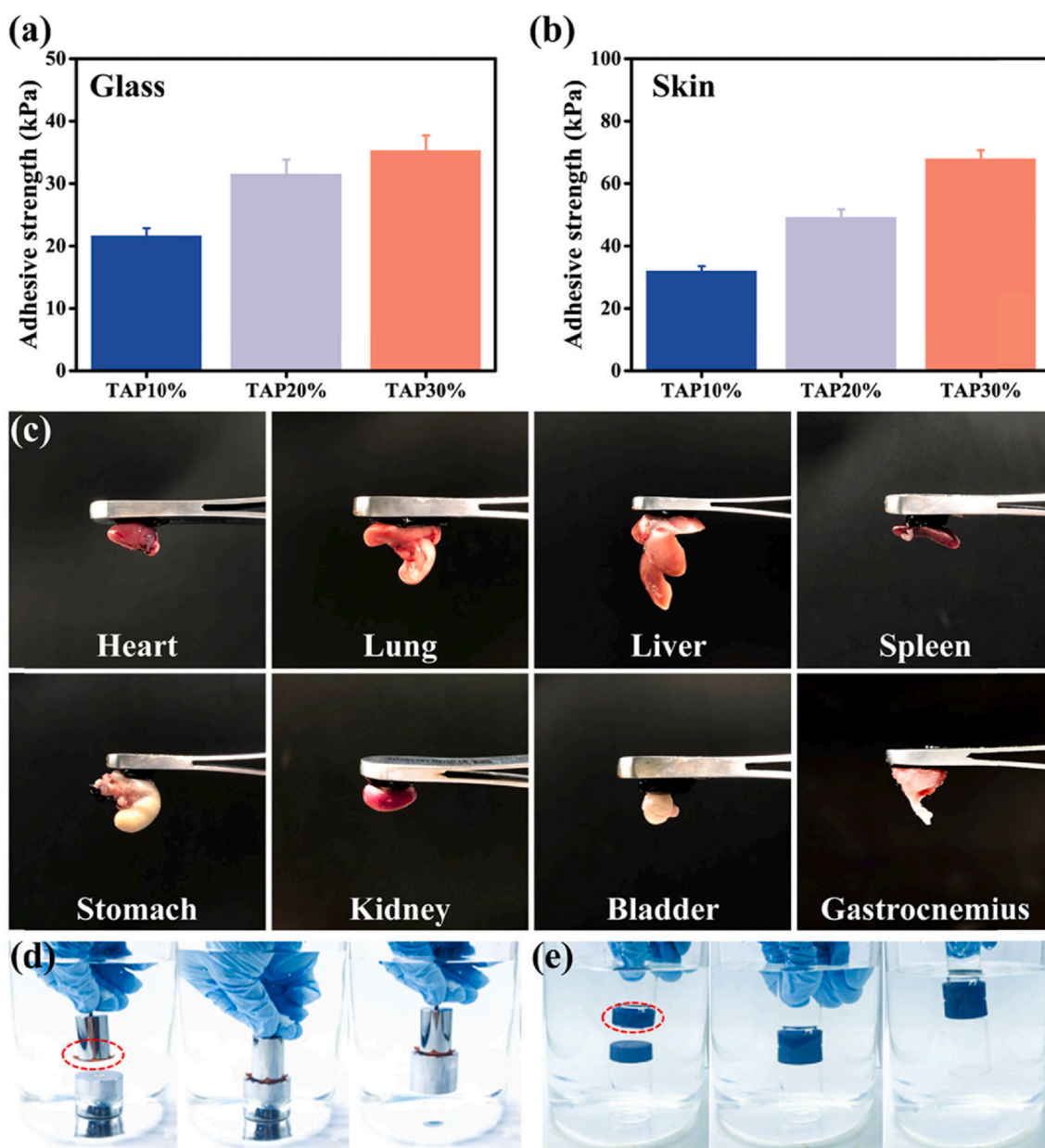


Fig. 2. Adhesive properties of TAP hydrogels. The lap-shear adhesive strength of TAP hydrogels on glass (a) and porcine skin (b). (c) Photographs of tissue adhesion situations of TAP30% hydrogel on 8 different organs of C57 BL/6 mice (heart, lung, liver, spleen, stomach, kidney, bladder, and gastrocnemius). Underwater adhesive behavior of TAP30% hydrogel with stainless steel weight (500 g) (d) and glass vial (e).

the beaker bottom, and a plastic bottle filled with water also could be lifted above water with TAP30% hydrogel (1 cm × 1 cm) attached to its cap, indicating the outstanding underwater adhesive capability of TAP30% hydrogel. The adhesion properties of TAP hydrogels with glass and porcine skin after water and blood contamination were also tested (Fig. S13). It was found that the adhesive strength of TAP hydrogel to glass and skin tissue was in the range of 15.33–42.41 kPa and 20.02–70.92 kPa, respectively. A slight decrease of the adhesive strength after water contamination was observed. These results demonstrated that TAP hydrogels could maintain their adhesive properties after water or blood contamination.

Supplementary video related to this article can be found at <https://doi.org/10.1016/j.bioactmat.2021.04.007>.

The increase of TA content not only introduced more catechol groups into TAP hydrogels but also enhanced the mechanical strength, both of which led to the increase of the adhesive strength.^[21, 30] The above results demonstrated that TAP hydrogels exhibit universal adhesive properties with various substrates and possess moist-resistant adhesive properties, which are desired for ideal wound dressing design.

2.4. In vitro antibacterial and antioxidant evaluation

It has been reported that TA shows broad-spectral antibacterial capability and could suppress the proliferation of both gram-positive and negative bacterial [5,31]. The mechanism of the antibacterial ability by TA is believed to be the interference of protein biosynthesis within bacterial cells [32]. Benefiting from this advantage of TA, TAP hydrogels also exhibited the inhibition ability of bacterial proliferation. After 12 h co-culture of TAP hydrogels with *E. coli* and *S. aureus*, the antibacterial capability was evaluated by bacterial colony formation counting method. As shown in Fig. 3a, PMI hydrogel did not affect the proliferation of bacterial as the control group, while TAP10%, TAP20%,

and TAP30% hydrogels exhibited 83%, 99%, and 99% killing efficiency against *E. coli* (Figs. 3b) and 99%, 99% and 99% against *S. aureus* (Fig. 3c), respectively, which was due to the sustained TA release. These results confirmed the excellent in vitro antibacterial property of TAP hydrogels against both gram-positive and gram-negative bacterial. Oxidative stress is known as a crucial predisposing factor in various pathology processes, such as inflammation, diabetes, Alzheimer's disease, Parkinson's disease, and even cancer [33]. The generation of excessive free radicals could cause tissue damage, promote inflammation reaction, and impair DNA structure [34]. The increased level of oxidative stress is also considered as an important reason for the infection and chronic wound formation in diabetic patients [35]. According to previous work, a wound dressing material with antioxidant ability could suppress inflammation reaction as well as promote wound healing [36]. TA is a nature-derived antioxidant factor and the large amounts of catechol groups within TA molecular could endow TAP hydrogels with excellent antioxidant activity. As shown in Fig. 3d, the in vitro antioxidative efficiency of TAP30% hydrogel was evaluated by 1-diphenyl-2-picrylhydrazyl (DPPH) free radicals scavenging test. It was found that the antioxidative efficiency gradually increased with the increase of TAP30% hydrogel concentration, and more than 90% free radical scavenging efficiency was observed at a relatively low concentration (0.05 mg/mL), which is similar to the scavenging efficiency of 5 mg/mL TA solution. These results demonstrated that TAP30% hydrogel shows outstanding free radical scavenging property and could be applied as an excellent antioxidant wound dressing to promote wound healing.

2.5. Hemostatic ability and wound closure evaluation

The hemostatic ability of TAP30% hydrogel was then evaluated using the rat hemorrhaging liver model (Fig. 4a). The liver bleeding was

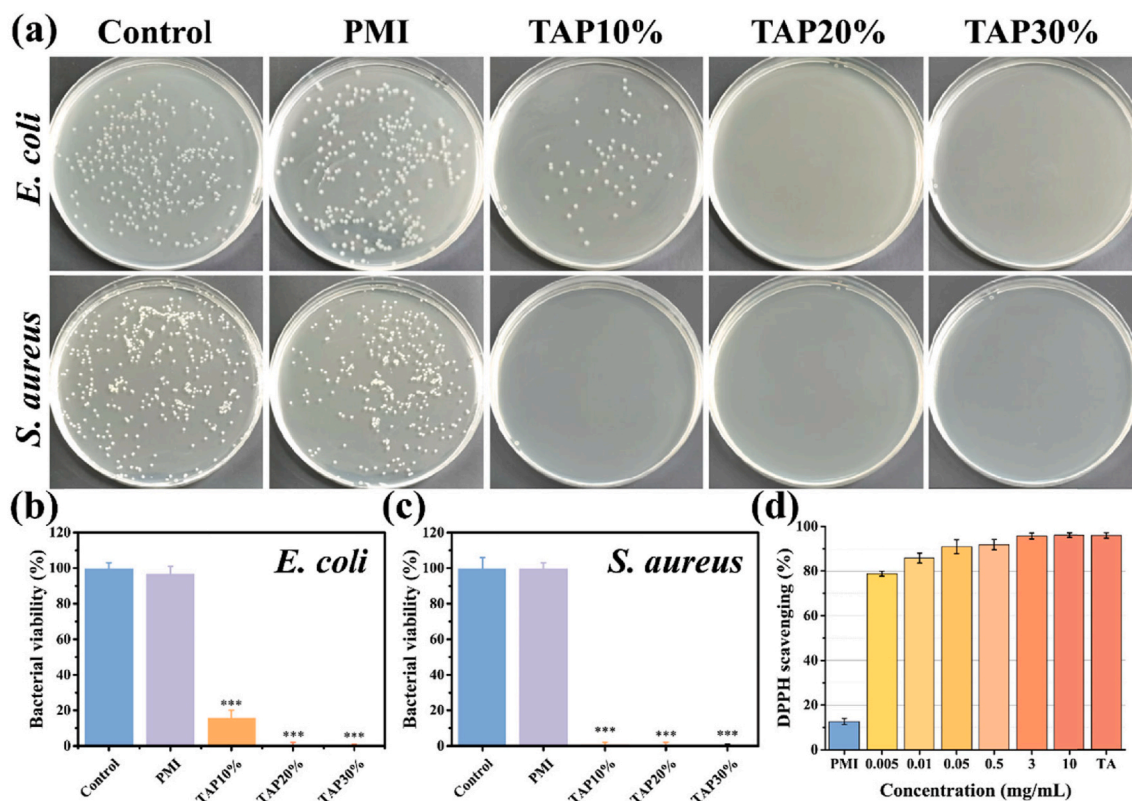


Fig. 3. Antibacterial and antioxidant properties of TAP hydrogels. (a) Photographs of the survival *E. coli* and *S. aureus* clones after co-cultured with PMI, TAP10%, TAP20%, and TAP30% hydrogels for 12 h. The corresponding quantitative bacterial survival rate of *E. coli* (b) and *S. aureus* (c). (d) Antioxidant property of TAP30% hydrogel evaluated by DPPH scavenging efficiency. * $P < 0.05$, ** $P < 0.01$, *** $P < 0.001$.

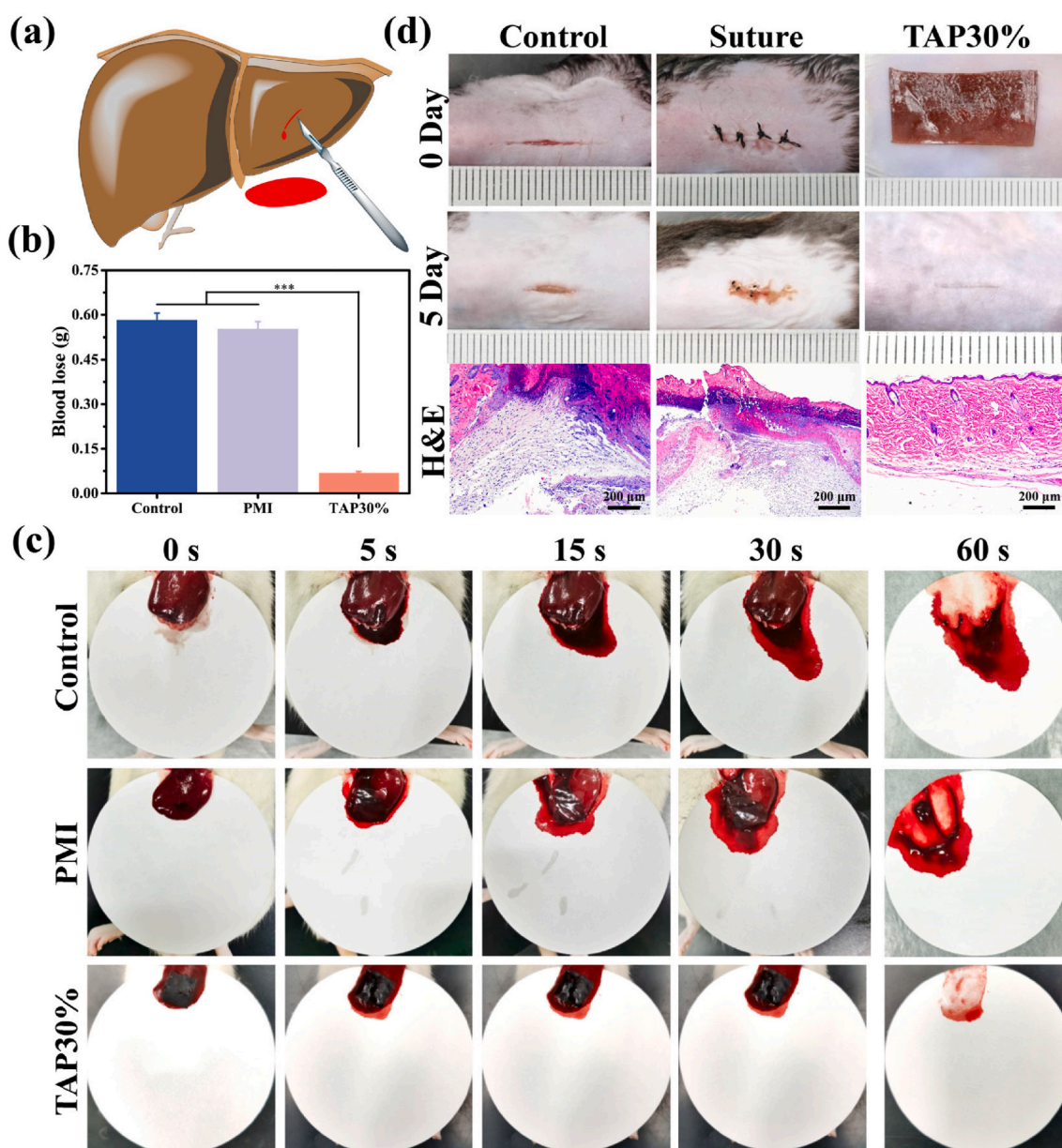


Fig. 4. Hemostatic and wound closure properties of TAP30% hydrogel. (a) Schematic illustration of rat hemorrhaging liver model (incision depth: 5 mm, length: 5 mm). (b) Total blood loss from rat liver wound after 60 s with different treatments. (c) Photographs of liver wound with different treatments at predetermined time intervals (0, 5, 15, 30, and 60 s). (d) Representative photographs and histological examination of full-thickness diabetic C57 BL/6 mice skin incision wound with different treatments.

controlled instantly, once the TAP30% hydrogel was adhered to the wound site, whereas the PMI and untreated groups showed obvious bleeding after 60 s. Detailedly, the untreated control group presented the most severe blood loss of 0.58 g, while the PMI hydrogel exhibited scarcely hemostatic capability with 0.55 g blood loss. Notably, TAP30% hydrogel significantly reduced blood loss (0.07 g, $P < 0.01$) compared with the other groups (Fig. 4b and c). The ideal hemostasis property of TAP30% hydrogel may be attributed to its moisture resist tissue adhesion ability. As shown in Movie S4, TAP30% hydrogel showed fast and reliable adhesion to rat liver and could act as a physical barrier to prevent further blood loss.

Supplementary video related to this article can be found at <https://doi.org/10.1016/j.bioactmat.2021.04.007>.

The *in vivo* promotion of wound closure by TAP30% hydrogel was tested on a full-thickness diabetic mice skin incision. A 1.5 cm incision wound was created on the dorsal skin of diabetic mice and treated by

TAP30% hydrogel. The surgical suture and untreated wound were used as control groups. As shown in Fig. 4d, the suture and non-treated control groups showed retained wound and scar tissue formation 5 days after surgery. These results may be attributed to the deformation of the skin caused by silk line in the suture group or tissue tensile of wound site in the control group. The uneven surface of two sides of the incision could compromise the healing process and lead to scar tissue formation, which is also commonly seen in clinical treatment [37]. Comparatively, the TAP30% hydrogel mediated excellent recovered skin surface, and only an inconspicuous mark was found on the incision site. With the treatment by TAP30% hydrogel, the incision surface was evenly attached, and the stretching of the tissue was restrained by TAP30% hydrogel with strong mechanical strength, which could lead to the fast recovery of the skin incision. Besides, hematoxylin and eosin (H&E) staining results showed that mild inflammatory cells infiltrated in control and suture groups, and the experimental group showed smooth and

intact tissue recovery, demonstrating the advantage of TAP hydrogel to promote wound healing.

2.6. *In vivo* wound healing performance of TAP30% hydrogel

Owing to promising mechanical strength and anti-fatigue property, adequate tissue adhesiveness, excellent antibacterial and antioxidant effects, and good hemostatic activity, TAP30% hydrogel was employed to evaluate the promotion of wound healing on full-thickness skin defect in diabetic mice. The diabetic mouse model was established through consecutive intraperitoneal injection of streptozotocin (STZ) for 5 days. Once the blood glucose level was stabilized above 300 mg dL⁻¹ (16.65

mmol/L) for 4 weeks, the mice were selected for wound healing evaluation. An 8 mm diameter skin punch wound was inoculated on the dorsal of the mice, which was subsequently treated with PMI hydrogel, Tegaderm film, TAP30% hydrogel, or left undressed. The gross inspection of the wound contraction in the four different groups on day 0, day 7, and day 14 were shown in Fig. 5a. It was found that TAP30% hydrogel showed faster wound recovery than the other three groups, and the wound almost disappeared after 14 days. To quantify the wound healing speed, the wound area was measured, and the results were presented in Fig. 5b. On the seventh day, the TAP30% hydrogel treated group showed 77% wound contraction, which was significantly faster than the control (51.7%), Tegaderm (51.9%), and PMI groups (64.5%). Moreover, the

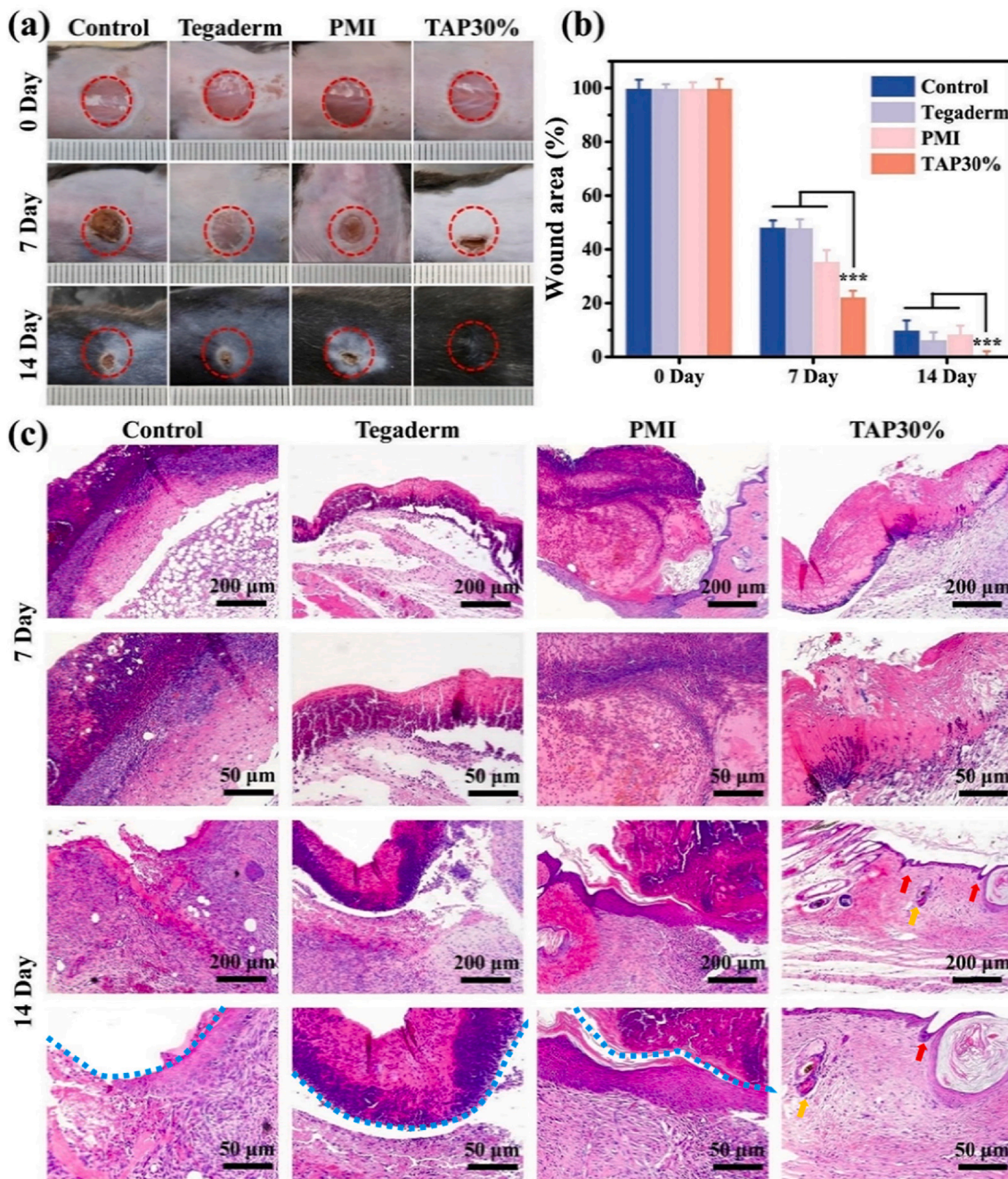


Fig. 5. The evaluation of diabetic wound healing. (a) Representative photographs of full-thickness skin wound healing on day 0, day 7, and day 14 for Tegaderm film, PMI hydrogel, TAP30% hydrogel, and control groups. (b) Wound contraction for Tegaderm film, PMI hydrogel, TAP30% hydrogel, and control groups. (c) Histological evaluation of regenerated skin tissues for Tegaderm film, PMI hydrogel, TAP30% hydrogel, and control groups on day 7 and day 14. Blue dotted line represents the residual blood crust. Red and yellow arrows represent hair follicles and sweat glands respectively.

blood crust completely fell off on the 14th day in the TAP30% hydrogel treated group, while there was still 10% unclosed wound area in the control group, 8.5% in the PMI hydrogel group, and 6.5% in the Tegaderm film treated group.

To reveal the promotion of wound healing by TAP30% hydrogel

from a histological perspective, H&E and Masson trichrome staining (MTS) were performed on regenerated skin tissues collected on day 7 and day 14. As demonstrated in Fig. 5c, inflammation response around the surgical site was observed in all four groups 7 days after surgery. However, the TAP30% hydrogel treated groups showed minimum

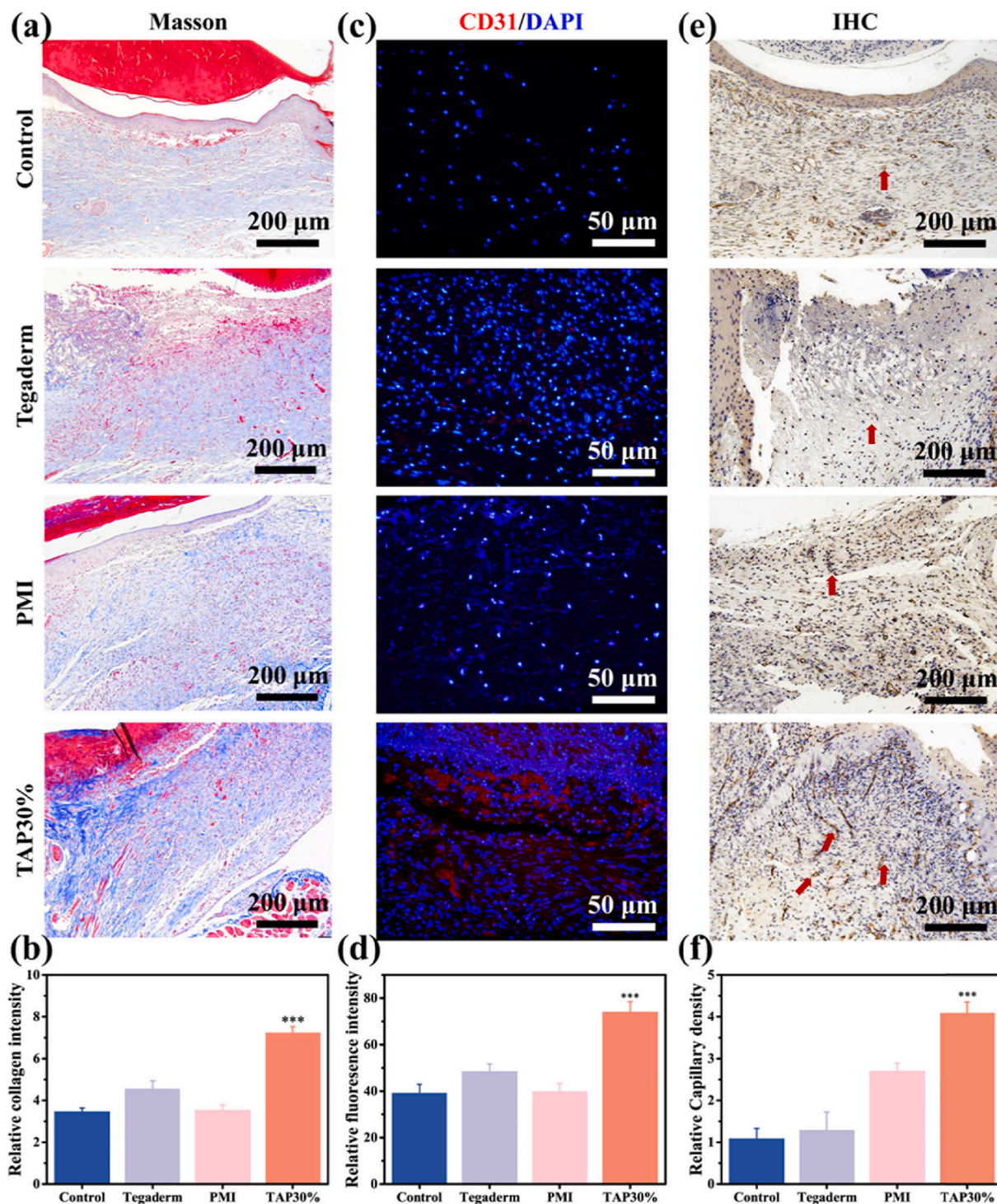


Fig. 6. Collagen deposition and angiogenesis evaluation of TAP30% hydrogel. (a) Masson staining of regenerated skin wounds for Tegaderm film, PMI hydrogel, TAP30% hydrogel, and control groups on day 14. (b) Quantitative analysis of relative percentage of collagen deposition coverage area for different groups. (c) Immunofluorescence staining of CD31 in regenerated skin tissue for Tegaderm film, PMI hydrogel, TAP30% hydrogel, and control groups on day 14. CD31 was labeled in red fluorescence and the cell nucleus was labeled in blue fluorescence. (d) Quantitative analysis of the relative percentage of CD31 fluorescence coverage area for different groups. (e) Immunohistochemical staining of CD31 in regenerated skin tissue for Tegaderm film, PMI hydrogel, TAP30% hydrogel, and control groups on day 14. Red arrows represent the location of blood vessels. (f) Relative capillary density in different groups. Mean ± SD (n = 3). *P < 0.05, **P < 0.01, ***P < 0.001.

inflammatory cell infiltration, which is due to the inflammation suppression by TA [38]. Meanwhile, Tegaderm, as well as PMI hydrogel, did not show significant difference in local inflammation reaction. On the 14th day, the TAP30% hydrogel treated group formed constant and almost intact epidermal tissue with cutaneous appendages regenerated within subcutaneous tissue, such as hair follicle and the sweat gland, which were marked with red and yellow arrows, respectively. Moreover, the blood crust (blue dotted lines) was still observed in the other three groups after 14 days of recovery as well as mild inflammatory response. MTS was also conducted on the 14th day after surgery to evaluate the collagen formation during the wound healing process. As shown in Fig. 6a and b, TAP30% hydrogel mediated the most collagen deposition, and there was no significant difference in collagen regeneration for the other three groups, indicating that the promotion of collagen deposition by TAP30% hydrogel accelerated the wound healing.

To further evaluate the revascularization mediated by TAP30% hydrogel in the wound healing process, immunofluorescence staining was performed to observe the newly formed vessel stained by the

vascular cell surface marker, platelet endothelial cell adhesion molecule-1 (CD31), with red fluorescence. Obvious red fluorescence was observed in the TAP30% treated group (Fig. 6c), and the relative fluorescence intensity was 1.8, 1.5, and 1.9 times higher than that by the control, Tegaderm film, and PMI hydrogel group, respectively (Fig. 6d). Interestingly, the CD31 expression in Tegaderm treated group was also higher than that of the control and PMI group. This may be attributed to the wound coverage provided by Tegaderm film, which led to less friction during the healing process. The immunohistochemical staining of CD31 was also performed, and the results in Fig. 6e showed a clear exhibition of the structure and distribution of blood vessels within the corium layer and subcutaneous tissue. The relative vessel density identified in the TAP30% treated group was much higher than that of the other three groups (Fig. 6f), which indicated a better pro-vascularization property of TAP30% hydrogel. The capillary regeneration was also evaluated at the molecular level. Vascular endothelial growth factor (VEGF) expression was further tested on the subcutaneous tissue around the wound area 7 days after surgery by ELISA test. As shown in Fig. 7a,

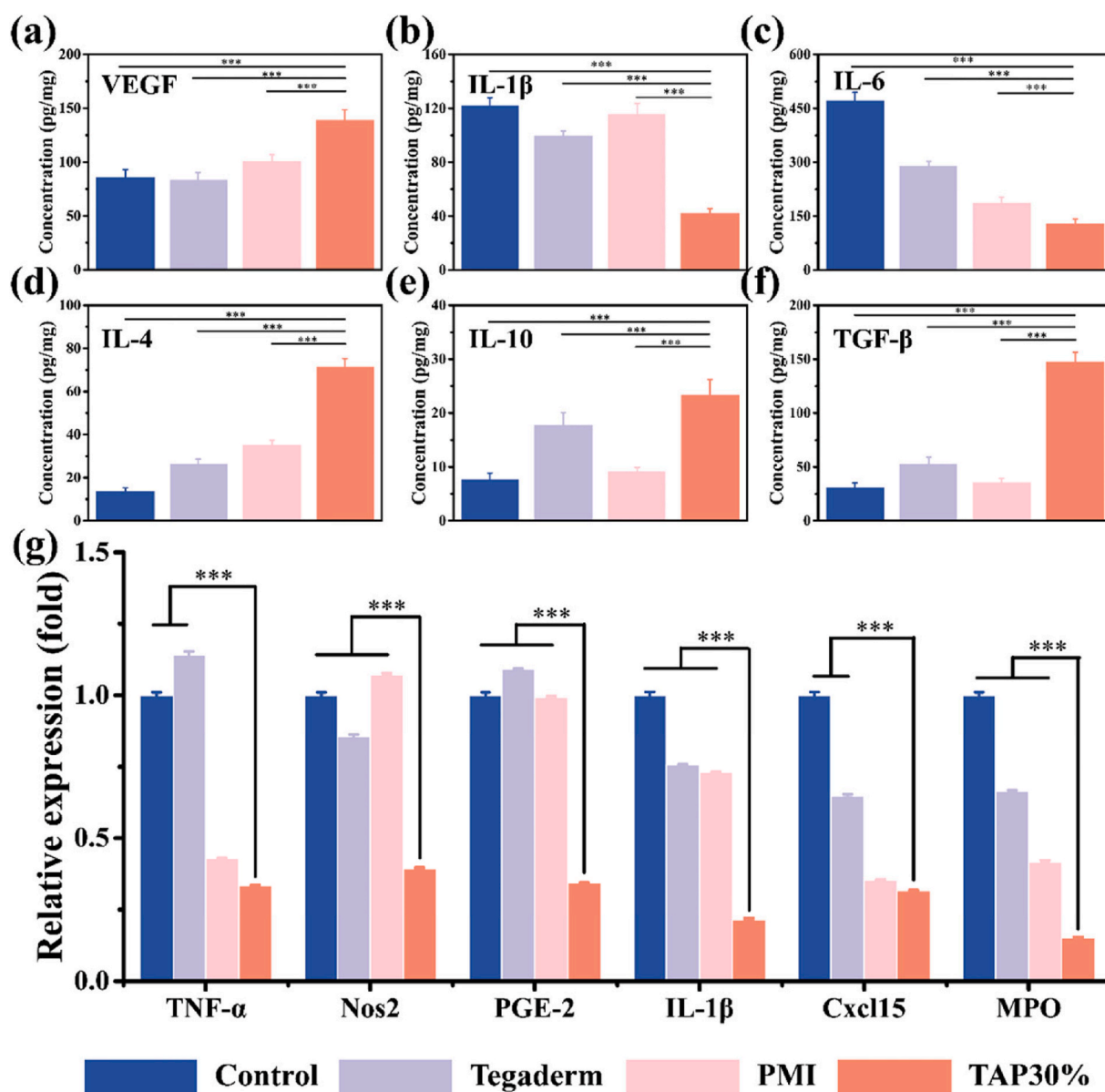


Fig. 7. Angiogenesis and anti-inflammation properties of TAP30% hydrogel. The expression intensity of inflammation and angiogenesis-related chemokines in full-thickness diabetic wound tissues with different treatments for 3 days were extracted and evaluated by ELISA (a–f) (n = 3). (g) The inflammation-related gene expression around full-thickness diabetic skin wound area was extracted and quantitatively evaluated by RT-PCR test (n = 3). *P < 0.05, **P < 0.01, ***P < 0.001.

the VEGF expression was significantly up-regulated in the TAP30% hydrogel treated group.

These results suggested that TAP30% hydrogel could significantly accelerate the skin wound healing through the regulation of inflammation, collagen deposition, and pro-vascularization.

2.7. Anti-inflammation evaluation

A variety of signal pathways can be activated by oxidative stress which can lead to the overexpression of chemokines, cell cycle regulatory molecules as well as inflammatory cytokines [39]. The up-regulated inflammation reaction is a major cause of prolonged wound closure in diabetic patients. To evaluate the anti-inflammation property of TAP30% hydrogel, ELISA examination was first performed on the samples collected from the wound site after 3 days of treatment. After the skin and subcutaneous tissue around the wound area were homogenized, the proteins were extracted for testing. The expression of the pro-inflammation factors interleukin-1 beta (IL-1 β) and interleukin 6 (IL-6) was significantly reduced in the TAP30% hydrogel treated group compared to the control, Tegaderm film, and PMI hydrogel group (Fig. 7b and c). Meanwhile, the expression of the anti-inflammatory cytokine, including interleukin 4 (IL-4), interleukin 10 (IL-10), and transforming growth factor-beta.

(TGF- β), was up-regulated mediated by TAP30% hydrogel (Fig. 7d–f), indicating obvious inflammation suppressive effect of

TAP30% hydrogel. The inflammation-related gene expression was also tested by RT-PCR to further demonstrate the advantage of TAP30% hydrogel. As shown in Fig. 7g, all inflammation factor expression including tumor necrosis factor-alpha (TNF- α), nitric oxide synthase 2 (Nos2), prostaglandin E2 (PGE-2), interleukin-1beta (IL-1 β), C-X-C motif chemokine 15 (Cxcl15), and myeloperoxidase (MPO) was down-regulated in the TAP30% hydrogel treated group. It was also noted that the expression of TNF- α , Cxcl15, and MPO was reduced in the Tegaderm film treated group compared to the control and PMI hydrogel treated group. These results proved the excellent anti-inflammation effect of TAP30% hydrogel.

2.8. In vivo degradation and systemic toxicity evaluation

The in vivo degradation of PMI and TAP hydrogels was evaluated through the subcutaneous implantation of the hydrogels into rats. The results showed that the degradation time was significantly extended in TAP30% hydrogel compared to PMI hydrogel, and TAP30% hydrogel can be completely cleared after 28 days of implantation (Fig. S14). Moreover, the long-term system toxicity of TAP30% was also evaluated by H&E staining of the tissues of heart, lung, liver, kidney, and spleen after 30 days of the treatment. Since PMI hydrogels showed good tissue biocompatibility and TA is a naturally derived antimicrobials molecule approved by the United States Food and Drug Administration (FDA) for human use [18,40], it is expected that TAP30% should show acceptable

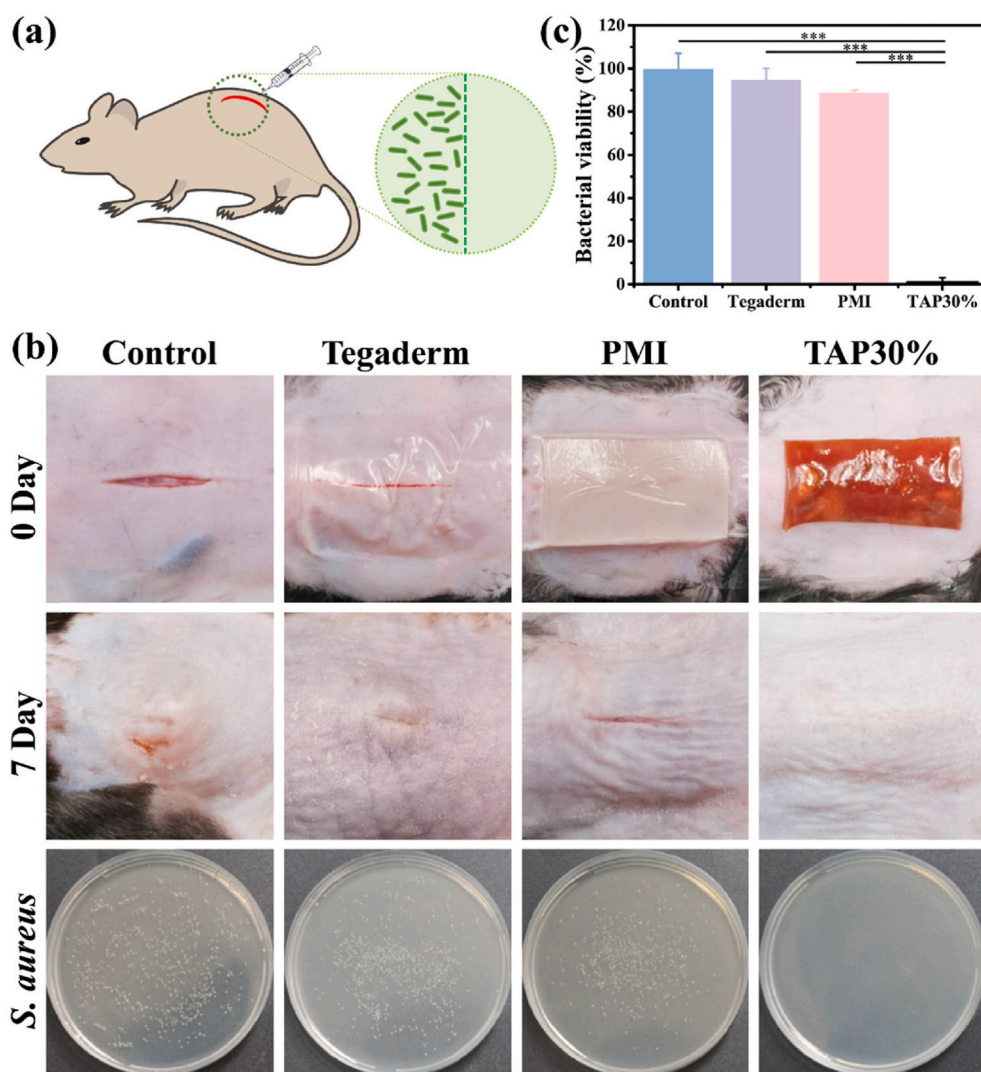


Fig. 8. In vivo antibacterial activity of TAP30% hydrogel (a) Schematic illustration of the construction of diabetic mice infectious wound model. (b) Representative photographs of infectious full-thickness mice dorsal skin wound on day 0 and day 7 with different treatments. The survival *S. aureus* clones on the agar plates from subcutaneous tissue of mice with different experimental conditions. (c) Quantitative bacterial survival rate of *S. aureus* extracted from control, Tegaderm, PMI, and TAP30% hydrogel treated groups. * $P < 0.05$, ** $P < 0.01$, *** $P < 0.001$.

safety for in vivo applications. As demonstrated in Fig. S15, the application of TAP30% hydrogel did not cause any damage in the main organs of mice compared to the control group, suggesting that TAP30% hydrogel is a good candidate for in vivo applications.

2.9. In vivo antibacterial evaluation

The bacterial infection is commonly found in diabetic chronic wounds due to the hyperglycemia, prolonged wound closure process, and increased inflammatory response [1b,16,17]. However, there were few works to report the treatment of infected diabetic wounds by hydrogel wound dressings. Herein, TAP30% hydrogel was employed to evaluate the treatment efficiency in the promotion of infected skin incision on diabetic C57 mice following published protocol [8b]. *S. aureus* is the most common pathogen on skin infections, which was injected in the skin incision to mimic the infected tissue in the clinic (Fig. 8a). As shown in Fig. 8b, the subcutaneous abscess was observed in control, Tegaderm film, and PMI hydrogel treated group 7 days after treatment, while the TAP30% hydrogel treated diabetic mice showed a smooth and almost intact skin healing without infectious symptom. Furthermore, the infected subcutaneous tissue was excised and homogenized to culture on the agar plate for standard plate counting after treatments. The photographs showed that there were few bacterial colonies observed in the TAP30% hydrogel treated group (Fig. 8b), and more than 99% reduction in CFU counting was achieved compared to the control, Tegaderm film, and PMI hydrogel treated groups (Fig. 8c). These results demonstrated that TAP30% hydrogel could be applied as an excellent antibacterial wound dressing for diabetic infected wound healing.

3. Conclusion

In summary, we developed a series of bioactive skin-mimicking hydrogels, TAP hydrogels, by soaking PMI film into TA solution with different concentrations. The TAP hydrogels exhibit ultra-strong mechanical strength, good self-recovery, and anti-fatigue performance, which could provide sufficient protection for wound areas and maintain the integrity of the dressings during the healing process. Moreover, the promising tissue adhesiveness and hemostatic activity were also achieved by TAP hydrogels. In vitro studies showed that TAP hydrogels efficiently inhibited the proliferation of *E. coli* and *S. aureus* as well as excellent antioxidant efficiency. In vivo results demonstrated that TAP30% not only accelerated the healing of skin incision and defect through the modulation of inflammation, promotion of collagen deposition, and vascularization, but also exhibited outstanding therapeutic efficiency with *S. aureus* infected skin incision on diabetic mice. Owing to the various advantages of TAP hydrogels, they may show vast potential as bioactive hydrogel band-aids for the treatment of different wounds for clinical applications.

4. Experimental section

4.1. Materials

Poly (ethylene glycol) (PEG) ($M_n = 10,000$), methylene diphenyl 4, 4-diisocyanate (MDI), imidazolidinyl urea (IU), dibutyltin dilaurate (DBTDL), *N,N*-dimethylformamide (DMF), and tannic acid (TA) were purchased from Aladdin Biological Technology Co., Ltd (Shanghai, China). All chemicals were analytical reagents and used as received. Streptozotocin (STZ, 98%) was purchased from Sigma-Aldrich.

4.2. Preparation of TAP hydrogels

TAP hydrogels were fabricated by soaking PMI dry films into TA solution. In brief, PMI hydrogel was first synthesized through polycondensation of PEG, MDI, and IU in the presence of DBTDL [18]. The

same amount of PMI dry film was then immersed in TA solution with different concentrations (10%, 20%, and 30%, w/v). A series of TAP hydrogels were obtained after 96 h swelling in TA solution. The synthetic protocol of PMI and TAP hydrogels was detailedly shown in Supplementary Material.

4.3. Mechanical properties of TAP hydrogels

The tensile test and consecutive loading-unloading test were employed to exam the mechanical properties of PMI and TAP hydrogels. The stress-strain curves were recorded, and the toughness and Young's modulus of each sample were calculated from the area under the stress-strain curve and the slope of the stress-strain curve. The dissipated energy of TAP30% hydrogels was calculated from the area between the loading-unloading curves. The self-recovery property of TAP30% hydrogel was tested through the loading-unloading test with different resting times. The experimental details are available in Supplementary Material.

4.4. Adhesion property of TAP hydrogels

The adhesion property of TAP hydrogels was tested on glass and porcine skin surfaces through a lap shear test as previously reported protocol [8b]. The underwater adhesion test of TAP30% was conducted in a glass baker filled with deionized water. The tissue adhesive property of the TAP30% hydrogel was tested on different mice tissue samples. The experimental details are available in Supplementary Material.

4.5. In vivo hemostasis and wound closure properties of TAP30% hydrogel

All animal protocols in this study were approved by the Ethical Committee of Xi'an Jiaotong University. The in vivo liver bleeding rat model was employed for hemostasis assay according to previously published research [19b]. The full-thickness skin incision model was employed to evaluate the wound closure ability of TAP30% hydrogel. The experimental details are available in Supplementary Material.

4.6. Full-thick skin wound healing evaluation

Type I diabetes was induced by successive streptozotocin (STZ) (Sigma-Aldrich, USA) intraperitoneal injection in C57BL/6 mice (male, 4 weeks). The widely used full-thickness dorsal skin defect model was employed to evaluate the wound healing ability of TAP30% hydrogel. The wound contraction rate, histopathologic examination, Masson trichrome staining, immunofluorescence, and immunohistochemical staining were used to study the wound healing, inflammation reaction, epithelial regeneration, collagen deposition, and revascularization properties of TAP30% hydrogel. The experimental details are available in Supplementary Material.

4.7. Anti-inflammation property of TAP30% hydrogel

Anti-inflammation property of TAP30% hydrogel was evaluated by ELISA and RT-PCR analysis. After different treatment for 3 days, 200 mg of fresh subcutaneous tissue around the wound area was weighted. The tissue samples were homogenized in a pre-cooled grinding tube before the total protein and RNA extraction. The expression levels of pro-inflammation protein IL-1 β and IL-6, anti-inflammation protein IL-4, IL-10, and TGF- β and VEGF were tested by ELISA. More pro-inflammation factors were evaluated by the RT-PCR. The details are available in Supplementary Material.

4.8. In vivo antibacterial evaluation

The infectious wound therapeutic ability of TAP30% hydrogel was

evaluated by treating *S. aureus* caused subcutaneous abscess on diabetic C57 mice model [8b]. The CFU of each group was photo-recorded and counted to evaluate the in vivo antibacterial property.

4.9. Statistical Analysis

All data are presented as mean \pm standard deviation ($*P < 0.05$, $**P < 0.01$, and $***P < 0.001$) and analyzed by the Student's t-test or one-way ANOVA followed by Tukey's post hoc test, in which $P < 0.05$ was considered statistical significance. SPSS 20.0 software (IBM, USA) and Origin Pro 2016 software (Origin Lab, USA) were used for data analysis and plotting.

Author contribution

Yuxuan Yang: Conceptualization, Formal analysis, Methodology, Writing - Original Draft **Xiaodan Zhao:** Visualization, Software, Methodology **Jing Yu:** Methodology **Xingxing Chen:** Software, Resources **Ruyue Wang:** Methodology **Mengyuan Zhang:** Investigation **Qiang Zhang:** Visualization **Yanfeng Zhang:** Supervision **Shuang Yang:** Project administration **Yilong Cheng:** Conceptualization, Supervision, Writing - review & editing, Project administration, Funding acquisition.

Declaration of competing interest

The authors declare no conflict of interest.

Acknowledgments

We thank Mr. Zijun Ren and Ms. Yanan Chen at Instrument Analysis Center of Xi'an Jiaotong University for their assistance with SEM test. Helpful support with Jianfeng Shi, Xinxin Wang, and Ruolin Liu at Key Laboratory of Shaanxi Province for Craniofacial Precision Medicine Research, Xi'an Jiaotong University, is highly appreciated. This work was financially supported by the following foundation: National Natural Science Foundation of China (NSFC 51803165), Natural Science Basic Research Plan in Shaanxi Province of China (2019JQ-167), Fundamental Research Funds for the Central Universities (xjj2018050 and xzy022019070) and "Young Talent Support Plan" of Xi'an Jiaotong University. We also thank the support from the Opening Project of Key Laboratory of Shaanxi Province for Craniofacial Precision Medicine Research, College of Stomatology, Xi'an Jiaotong University (2019LHM-KFKT007). Yuxuan Yang and Xiaodan Zhao contributed equally to this work.

Appendix A. Supplementary data

Supplementary data to this article can be found online at <https://doi.org/10.1016/j.bioactmat.2021.04.007>.

References

- (a) Y.K. Wu, N.C. Cheng, C.M. Cheng, Biofilms in chronic wounds: pathogenesis and diagnosis, *Trends Biotechnol.* 37 (2019) 505, <https://doi.org/10.1016/j.tibtech.2018.10.011>;
- (b) W.J. Jeffcoate, K.G. Harding, Diabetic foot ulcers, *Lancet* 361 (2003) 1545, [https://doi.org/10.1016/S0140-6736\(03\)13169-8](https://doi.org/10.1016/S0140-6736(03)13169-8).
- L. The, Diabetes: a dynamic disease, *Lancet* 389 (2017), [https://doi.org/10.1016/S0140-6736\(17\), 31537-4](https://doi.org/10.1016/S0140-6736(17), 31537-4).
- L.I. Moura, A.M. Dias, E. Carvalho, H.C. de Sousa, Recent advances on the development of wound dressings for diabetic foot ulcer treatment—a review, *Acta Biomater.* 9 (2013) 7093, <https://doi.org/10.1016/j.actbio.2013.03.033>.
- A.E. Boniakowski, A.S. Kimball, B.N. Jacobs, S.L. Kunkel, K.A. Gallagher, Macrophage-mediated inflammation in normal and diabetic wound healing, *J. Immunol.* 199 (2017) 17, <https://doi.org/10.4049/jimmunol.1700223>.
- X. Zhao, H. Wu, B. Guo, R. Dong, Y. Qiu, P.X. Ma, Antibacterial anti-oxidant electroactive injectable hydrogel as self-healing wound dressing with hemostasis and adhesiveness for cutaneous wound healing, *Biomaterials* 122 (2017) 34, <https://doi.org/10.1016/j.biomaterials.2017.01.011>.
- L. Shi, X. Liu, W. Wang, L. Jiang, S. Wang, A self-pumping dressing for draining excessive biofluid around wounds, *Adv. Mater.* 31 (2019), e1804187, <https://doi.org/10.1002/adma.201804187>.
- (a) L.S. Wang, P.Y. Chow, D.C.W. Tan, W.D. Zhang, Y.Y. Yang, Nanostructured and transparent polymer membranes with thermosensitivity for wound dressing and cell grafting, *Adv. Mater.* 16 (2004) 1790, <https://doi.org/10.1002/adma.200400602>;
- (b) F. Bao, G. Pei, Z.C. Wu, H. Zhuang, Z.W.B. Zhang, Z.G. Huan, C.T. Wu, J. Chang, Bioactive self-pumping composite wound dressings with micropore array modified Janus membrane for enhanced diabetic wound healing, *Adv. Funct. Mater.* 30 (2020), <https://doi.org/10.1002/adfm.202005422>.
- (a) W.C. Huang, R. Ying, W. Wang, Y. Guo, Y. He, X. Mo, C. Xue, X. Mao, A macroporous hydrogel dressing with enhanced antibacterial and anti-inflammatory capabilities for accelerated wound healing, *Adv. Funct. Mater.* 30 (2020) 10, <https://doi.org/10.1002/adfm.202000644>;
- (b) X. Zhao, Y.P. Liang, Y. Huang, J.H. He, Y. Han, B.L. Guo, Physical double-network hydrogel adhesives with rapid shape adaptability, fast self-healing, antioxidant and NIR/pH stimulus-responsiveness for multidrug-resistant bacterial infection and removable wound dressing, *Adv. Funct. Mater.* 30 (2020) 18, <https://doi.org/10.1002/adfm.201910748>;
- (c) S. Liu, J. Yu, Q. Zhang, H. Lu, X. Qiu, D. Zhou, Y. Qi, Y. Huang, Dual cross-linked HHA hydrogel supplies and regulates MPhi2 for synergistic improvement of immunocompromise and impaired angiogenesis to enhance diabetic chronic wound healing, *Biomacromolecules* 21 (2020) 3795, <https://doi.org/10.1021/acs.biomac.0c00891>;
- (d) S. Liu, Q. Zhang, J. Yu, N. Shao, H. Lu, J. Guo, X. Qiu, D. Zhou, Y. Huang, Absorbable thioether grafted hyaluronic acid nanofibrous hydrogel for synergistic modulation of inflammation microenvironment to accelerate chronic diabetic wound healing, *Adv. Healthc. Mater.* 9 (2020), e2000198, <https://doi.org/10.1002/adhm.202000198>.
- Z. Qian, H. Wang, Y. Bai, Y. Wang, L. Tao, Y. Wei, Y. Fan, X. Guo, H. Liu, Improving chronic diabetic wound healing through an injectable and self-healing hydrogel with platelet-rich plasma release, *ACS Appl. Mater. Interfaces* 12 (2020) 55659, <https://doi.org/10.1021/acsami.0c17142>.
- L. Wang, J. Yang, X. Yang, Q. Hou, S. Liu, W. Zheng, Y. Long, X. Jiang, Mercaptophenylboronic acid-activated gold nanoparticles as nanoantibiotics against multidrug-resistant bacteria, *ACS Appl. Mater. Interfaces* (2020), <https://doi.org/10.1021/acsami.0c12597>. DOI: 10.1021/acsami.0c12597.
- Z. Ahmadian, A. Correia, M. Hasany, P. Figueiredo, F. Dobakhti, M.R. Eskandari, S. H. Hosseini, R. Abiri, S. Khorshid, J. Hirvonen, H.A. Santos, M.-A. Shahbazi, A hydrogen-bonded extracellular matrix-mimicking bactericidal hydrogel with radical scavenging and hemostatic function for pH-responsive wound healing acceleration, *Adv. Healthc. Mater.* (2020), <https://doi.org/10.1002/adhm.202001122>.
- T. Chen, Y.J. Chen, H.U. Rehman, Z. Chen, Z. Yang, M. Wang, H. Li, H.Z. Liu, Ultratough, self-healing, and tissue-adhesive hydrogel for wound dressing, *ACS Appl. Mater. Interfaces* 10 (2018) 33523, <https://doi.org/10.1021/acsami.8b10064>.
- (a) C.K. Xuan, L.J. Hao, X.M. Liu, Y. Zhu, H.S. Yang, Y.P. Ren, L. Wang, T. Fujie, H. K. Wu, Y.H. Chen, X.T. Shi, C.B. Mao, Wet-adhesive, haemostatic and antimicrobial bilayered composite nanosheets for sealing and healing soft-tissue bleeding wounds, *Biomaterials* 252 (2020) 13, <https://doi.org/10.1016/j.biomaterials.2020.120018>;
- (b) Q. Peng, J. Chen, Z. Zeng, T. Wang, L. Xiang, X. Peng, J. Liu, H. Zeng, Adhesive coacervates driven by hydrogen-bonding interaction, *Small* 16 (2020), e2004132, <https://doi.org/10.1002/smll.202004132>.
- M. He, L. Sun, X. Fu, S.P. McDonough, C.-C. Chu, Biodegradable amino acid-based poly(ester amine) with tunable immunomodulating properties and their in vitro and in vivo wound healing studies in diabetic rats' wounds, *Acta Biomater.* 84 (2019) 114, <https://doi.org/10.1016/j.actbio.2018.11.053>.
- D.G. Armstrong, J.R. Ingelfinger, A.J.M. Boulton, S.A. Bus, Diabetic foot ulcers and their recurrence, *N. Engl. J. Med.* 376 (2017) 2367, <https://doi.org/10.1056/NEJMr1615439>.
- V. Falanga, Wound healing and its impairment in the diabetic foot, *Lancet* 366 (2005) 1736, [https://doi.org/10.1016/S0140-6736\(05\)67700-8](https://doi.org/10.1016/S0140-6736(05)67700-8).
- A.J. Boulton, L. Vileikyte, G. Ragnarson-Tennvall, J. Apelqvist, The global burden of diabetic foot disease, *Lancet* 366 (2005) 1719, [https://doi.org/10.1016/S0140-6736\(05\)67698-2](https://doi.org/10.1016/S0140-6736(05)67698-2).
- Y. Yang, X. Zhao, J. Yu, X. Chen, X. Chen, C. Cui, J. Zhang, Q. Zhang, Y. Zhang, S. Wang, Y. Cheng, H-bonding supramolecular hydrogels with promising mechanical strength and shape memory properties for postoperative antiadhesion application, *ACS Appl. Mater. Interfaces* 12 (2020) 34161, <https://doi.org/10.1021/acsami.0c07753>.
- (a) N. Ninan, A. Forget, V.P. Shastri, N.H. Voelcker, A. Blencowe, Antibacterial and anti-inflammatory pH-responsive tannic acid-carboxylated agarose composite hydrogels for wound healing, *ACS Appl. Mater. Interfaces* 8 (2016) 28511, <https://doi.org/10.1021/acsami.6b10491>;
- (b) J.Y. Liu, Y. Hu, L. Li, C. Wang, J. Wang, Y. Li, D. Chen, X. Ding, C. Shen, F. J. Xu, Biomass-derived multilayer-structured microparticles for accelerated hemostasis and bone repair, *Adv. Sci.* 7 (2020) 2002243, <https://doi.org/10.1002/advs.202002243>;
- (c) A. Shukla, J.C. Fang, S. Puranam, F.R. Jensen, P.T. Hammond, Hemostatic multilayer coatings, *Adv. Mater.* 24 (2012) 492, <https://doi.org/10.1002/adma.201103794>;
- (d) W. Sun, H. Jiang, X. Wu, Z. Xu, C. Yao, J. Wang, M. Qin, Q. Jiang, W. Wang, D. Shi, Y. Cao, Strong dual-crosslinked hydrogels for ultrasound-triggered drug

- delivery, *Nano Res.* 12 (2019) 115, <https://doi.org/10.1007/s12274-018-2188-4>;
- (e) W. Chen, N. Li, Y. Ma, M.L. Minus, K. Benson, X. Lu, X. Wang, X. Ling, H. Zhu, Superstrong and tough hydrogel through physical cross-linking and molecular alignment, *Biomacromolecules* 20 (2019) 4476, <https://doi.org/10.1021/acs.biomac.9b01223>.
- [20] F. Sun, Y. Bu, Y. Chen, F. Yang, J. Yu, D. Wu, An injectable and instant self-healing medical adhesive for wound sealing, *ACS Appl. Mater. Interfaces* 12 (2020) 9132, <https://doi.org/10.1021/acsami.0c01022>.
- [21] (a) Y.N. Chen, L. Peng, T. Liu, Y. Wang, S. Shi, H. Wang, Poly(vinyl alcohol)-tannic acid hydrogels with excellent mechanical properties and shape memory behaviors, *ACS Appl. Mater. Interfaces* 8 (2016) 27199, <https://doi.org/10.1021/acsami.6b08374>;
- (b) J. Wang, F. Tang, Y. Wang, Q. Lu, S. Liu, L. Li, Self-healing and highly stretchable gelatin hydrogel for self-powered strain sensor, *ACS Appl. Mater. Interfaces* 12 (2020) 1558, <https://doi.org/10.1021/acsami.9b18646>;
- (c) R. Xu, S. Ma, P. Lin, B. Yu, F. Zhou, W. Liu, High strength astringent hydrogels using protein as the building block for physically cross-linked multi-network, *ACS Appl. Mater. Interfaces* 10 (2018) 7593, <https://doi.org/10.1021/acsami.7b04290>;
- (d) X. Du, L. Wu, H. Yan, L. Qu, L. Wang, X. Wang, S. Ren, D. Kong, L. Wang, Multifunctional hydrogel patch with toughness, tissue adhesiveness, and antibacterial activity for sutureless wound closure, *ACS Biomater. Sci. Eng.* 5 (2019) 2610, <https://doi.org/10.1021/acsbomaterials.9b00130>.
- [22] D. Zhang, Z. Xu, H. Li, C. Fan, C. Cui, T. Wu, M. Xiao, Y. Yang, J. Yang, W. Liu, Fabrication of strong hydrogen-bonding induced coacervate adhesive hydrogels with antibacterial and hemostatic activities, *Biomater. Sci.* 8 (2020) 1455, <https://doi.org/10.1039/c9bm02029b>.
- [23] (a) Y. Dong, A. Bazrafshan, A. Pokutta, F. Sulejmani, W. Sun, J.D. Combs, K. C. Clarke, K. Salaita, Chameleon-inspired strain-accommodating smart skin, *ACS Nano* 13 (2019) 9918, <https://doi.org/10.1021/acsnano.9b04231>;
- (b) R. Fu, L. Tu, Y. Zhou, L. Fan, F. Zhang, Z. Wang, J. Xing, D. Chen, C. Deng, G. Tan, P. Yu, L. Zhou, C. Ning, A tough and self-powered hydrogel for artificial skin, *Chem. Mater.* 31 (2019) 9850, <https://doi.org/10.1021/acs.chemmater.9b04041>.
- [24] (a) J.M. Lord, M.J. Midwinter, Y.F. Chen, A. Belli, K. Brohi, E.J. Kovacs, L. Koenderman, P. Kubers, R.J. Lilford, The systemic immune response to trauma: an overview of pathophysiology and treatment, *Lancet* 384 (2014) 1455, [https://doi.org/10.1016/S0140-6736\(14\)60687-5](https://doi.org/10.1016/S0140-6736(14)60687-5);
- (b) P.G. Bowler, B.I. Duerden, D.G. Armstrong, Wound microbiology and associated approaches to wound management, *Clin. Microbiol. Rev.* 14 (2001) 244, <https://doi.org/10.1128/CMR.14.2.244-269.2001>.
- [25] C. Wang, H. Zhou, H. Niu, X. Ma, Y. Yuan, H. Hong, C. Liu, Tannic acid-loaded mesoporous silica for rapid hemostasis and antibacterial activity, *Biomater. Sci.* 6 (2018) 3318, <https://doi.org/10.1039/c8bm00837j>.
- [26] T.H. Chang, K. Li, H. Yang, P.Y. Chen, Multifunctionality and mechanical actuation of 2D materials for skin-mimicking capabilities, *Adv. Mater.* 30 (2018), e1802418, <https://doi.org/10.1002/adma.201802418>.
- [27] (a) Y.P. Zheng, Y.K.C. Choi, K. Wong, S. Chan, A.F.T. Mak, Biomechanical assessment of plantar foot tissue in diabetic patients using an ultrasound indentation system, *Ultrasound Med. Biol.* 26 (2000) 451, [https://doi.org/10.1016/S0301-5629\(99\)00163-5](https://doi.org/10.1016/S0301-5629(99)00163-5);
- (b) C.T. McKee, J.A. Last, P. Russell, C.J. Murphy, Indentation versus tensile measurements of Young's modulus for soft biological tissues, *Tissue Eng. B Rev.* 17 (2011) 155, <https://doi.org/10.1089/ten.TEB.2010.0520>;
- (c) S.F. Leung, Y. Zheng, C.Y. Choi, S.S. Mak, S.K. Chiu, B. Zee, A.F. Mak, Quantitative measurement of post-irradiation neck fibrosis based on the young modulus: description of a new method and clinical results, *Cancer* 95 (2002) 656, <https://doi.org/10.1002/cncr.10700>.
- [28] X. Dai, Y. Zhang, L. Gao, T. Bai, W. Wang, Y. Cui, W. Liu, A mechanically strong, highly stable, thermoplastic, and self-healable supramolecular polymer hydrogel, *Adv. Mater.* 27 (2015) 3566, <https://doi.org/10.1002/adma.201500534>.
- [29] E. Lamers, T.H.S. van Kempen, F.P.T. Baaijens, G.W.M. Peter, C.W.J. Oomens, Large amplitude oscillatory shear properties of human skin, *J. Mech. Behav. Biomed. Mater.* 28 (2013) 462, <https://doi.org/10.1016/j.jmbbm.2013.01.024>.
- [30] (a) J. Shin, J.S. Lee, C. Lee, H.J. Park, K. Yang, Y. Jin, J.H. Ryu, K.S. Hong, S. H. Moon, H.M. Chung, H.S. Yang, S.H. Um, J.W. Oh, D.I. Kim, H. Lee, S.W. Cho, Tissue adhesive catechol-modified hyaluronic acid hydrogel for effective, minimally invasive cell therapy, *Adv. Funct. Mater.* 25 (2015) 3814, <https://doi.org/10.1002/adfm.201500006>;
- (b) C. Cui, C. Fan, Y. Wu, M. Xiao, T. Wu, D. Zhang, X. Chen, B. Liu, Z. Xu, B. Qu, W. Liu, Water-Triggered hyperbranched polymer universal adhesives: from strong underwater adhesion to rapid sealing hemostasis, *Adv. Mater.* 31 (2019), e1905761, <https://doi.org/10.1002/adma.201905761>;
- (c) J. Yang, R. Bai, B. Chen, Z. Suo, Hydrogel adhesion: a supramolecular synergy of chemistry, topology, and mechanics, *Adv. Funct. Mater.* 30 (2019) 1901693, <https://doi.org/10.1002/adfm.201901693>;
- (d) R. Wang, J. Li, W. Chen, T. Xu, S. Yun, Z. Xu, Z. Xu, T. Sato, B. Chi, H. Xu, A biomimetic mussel-inspired e-Poly-L-lysine hydrogel with robust tissue-anchor and anti-infection capacity, *Adv. Funct. Mater.* 27 (2017) 1604894, <https://doi.org/10.1002/adfm.201604894>;
- (e) D. Lee, H. Hwang, J.-S. Kim, J. Park, D. Youn, D. Kim, J. Hahn, M. Seo, H. Lee, VATA: a poly(vinyl alcohol)- and tannic acid-based nontoxic underwater adhesive, *ACS Appl. Mater. Interfaces* 12 (2020) 20933, <https://doi.org/10.1021/acsami.0c02037>.
- [31] Y. Wang, Y. Yang, Y. Shi, H. Song, C. Yu, Antibiotic-free antibacterial strategies enabled by nanomaterials: progress and perspectives, *Adv. Mater.* 32 (2020), e1904106, <https://doi.org/10.1002/adma.201904106>.
- [32] N.S. Khan, A. Ahmad, S.M. Hadi, Anti-oxidant, pro-oxidant properties of tannic acid and its binding to DNA, *Chem. Biol. Interact.* 125 (2000) 177, [https://doi.org/10.1016/S0009-2797\(00\)00143-5](https://doi.org/10.1016/S0009-2797(00)00143-5).
- [33] (a) C. Gorrini, I.S. Harris, T.W. Mak, Modulation of oxidative stress as an anticancer strategy, *Nat. Rev. Drug Discov.* 12 (2013) 931, <https://doi.org/10.1038/nrd4002>;
- (b) H. Sies, Oxidative stress: a concept in redox biology and medicine, *Redox Biol.* 4 (2015) 180, <https://doi.org/10.1016/j.redox.2015.01.002>;
- (c) A. van der Pol, W.H. van Gilst, A.A. Voors, P. van der Meer, Treating oxidative stress in heart failure: past, present and future, *Eur. J. Heart Fail.* 21 (2019) 425, <https://doi.org/10.1002/ehfj.1320>.
- [34] (a) J.J. Yang, C. Wang, X.L. Liu, Y. Yin, Y.H. Ma, Y.F. Gao, Y.Z. Wang, Z.D. Lu, Y. J. Song, Gallium-carbenicillin framework coated defect-rich hollow TiO₂ as a photocatalyzed oxidative stress amplifier against complex infections, *Adv. Funct. Mater.* 30 (2020), <https://doi.org/10.1002/adfm.202004861>;
- (b) M. Dizdaroglu, P. Jaruga, M. Birincioğlu, H. Rodriguez, Free radical-induced damage to DNA: mechanisms and measurement, *Free Radic. Biol. Med.* 32 (2002) 1102, [https://doi.org/10.1016/S0891-5849\(02\)00826-2](https://doi.org/10.1016/S0891-5849(02)00826-2).
- [35] (a) D.J. Betteridge, What is oxidative stress? *Metabolism* 49 (2000) 3, [https://doi.org/10.1016/S0026-0495\(00\)80077-3](https://doi.org/10.1016/S0026-0495(00)80077-3);
- (b) B.S. Karam, A. Chavez-Moreno, W. Koh, J.G. Akar, F.G. Akar, Oxidative stress and inflammation as central mediators of atrial fibrillation in obesity and diabetes, *Cardiovasc. Diabetol.* 16 (2017) 120, <https://doi.org/10.1186/s12933-017-0604-9>;
- (c) A.C. Maritim, R.A. Sanders, J.B. Watkins 3rd, Diabetes, oxidative stress, and antioxidants: a review, *J. Biochem. Mol. Toxicol.* 17 (2003) 24, <https://doi.org/10.1002/jbt.10058>.
- [36] W.C. Huang, R. Ying, W. Wang, Y. Guo, Y. He, X. Mo, C. Xue, X. Mao, Macroporous hydrogel dressing: a macroporous hydrogel dressing with enhanced antibacterial and anti-inflammatory capabilities for accelerated wound healing, *Adv. Funct. Mater.* 30 (2020), <https://doi.org/10.1002/adfm.202070132>.
- [37] S. Korntner, C. Lehner, R. Gehwolf, A. Wagner, M. Grutz, N. Kunkel, H. Tempfer, A. Traweger, Limiting angiogenesis to modulate scar formation, *Adv. Drug Deliv. Rev.* 146 (2019) 170, <https://doi.org/10.1016/j.addr.2018.02.010>.
- [38] (a) X. Li, P. Gao, J. Tan, K. Xiong, M.F. Maitz, C. Pan, H. Wu, Y. Chen, Z. Yang, N. Huang, Assembly of metal-phenolic/catecholamine networks for synergistically anti-inflammatory, antimicrobial, and anticoagulant coatings, *ACS Appl. Mater. Interfaces* 10 (2018) 40844, <https://doi.org/10.1021/acsami.8b14409>;
- (b) D. Pham-Hua, L.E. Padgett, B. Xue, B. Anderson, M. Zeiger, J.M. Barra, M. Bethea, C.S. Hunter, V. Kozlovskaya, E. Kharlampieva, H.M. Tse, Islet encapsulation with polyphenol coatings decreases pro-inflammatory chemokine synthesis and T cell trafficking, *Biomaterials* 128 (2017) 19, <https://doi.org/10.1016/j.biomaterials.2017.03.002>.
- [39] S. Reuter, S.C. Gupta, M.M. Chaturvedi, B.B. Aggarwal, Oxidative stress, inflammation, and cancer: how are they linked? *Free Radic. Biol. Med.* 49 (2010) 1603, <https://doi.org/10.1016/j.freeradbiomed.2010.09.006>.
- [40] H. Tan, J. Sun, D. Jin, J. Song, M. Lei, A. Antoshin, X. Chen, M. Yin, X. Qu, C. Liu, Coupling PEG-LZM polymer networks with polyphenols yields suturable biohydrogels for tissue patching, *Biomater. Sci.* 8 (2020) 3334, <https://doi.org/10.1039/d0bm00429d>.